SUPPORTING INFORMATION

Ligand Rigidity as a Design Principle for Planar Pentacoordinate Fluorine

Li-Xia Bai,[a] Ya-Xuan Cheng,[a] Fernando Martínez-Villarino,[b] Luz Diego,[c] Jin-Chang Guo,[a*] and Gabriel Merino.[b*]

[a]Institute of Molecular Science, Shanxi University, Taiyuan 030006, China.

[b]Departamento de Física Aplicada, Centro de Investigación y de Estudios Avanzados, Unidad Mérida. Km 6 Antigua Carretera a Progreso. Apdo. Postal 73, Cordemex, 97310, Mérida, Yucatan, México.

[c]Doctorado en Fisicoquímica Molecular, Facultad de Ciencias Exactas, Universidad Andres Bello, Av. República 275, Santiago, Chile.

[*]E-mail: guojc@sxu.edu.cn; gmerino@cinvestav.mx

COMPUTATIONAL DETAILS

The potential energy surface (PES) of $FZn_5O_5^-$ was explored using the Coalescence Kick algorithm.[1] This global search strategy was applied at the PBE0/def2-SVP level to ensure broad sampling of the configurational space.[2,3] Approximately 4000 initial geometries were generated and optimized, evenly distributed between singlet and triplet spin states. In addition to the automated global search, selected low-energy structures were manually constructed to improve coverage of chemically reasonable motifs. The lowest-lying isomers obtained from both approaches were subsequently reoptimized at the PBE0-D3(BJ)/def2-TZVPP level.[4] Harmonic vibrational frequency calculations at the same level were performed to characterize the stationary points and confirm that the reported structures correspond to true minima on the PES. Relative energies were evaluated using single-point calculations at the CCSD(T)/def2-TZVPP level on PBE0-D3(BJ)/def2-TZVPP geometries.[5] Zero-point energy corrections were included and evaluated at the PBE0-D3(BJ)/def2-TZVPP level. T_1 diagnostic values confirm the validity of a single-reference description for both singlet and triplet states.

Dynamic stability was assessed using Born–Oppenheimer molecular dynamics simulations.[6] Simulations were carried out at the PBE0/def2-SVP level and used to monitor the structural integrity of the global minimum over finite simulation times.

Chemical bonding was analyzed using complementary theoretical approaches. Natural bond orbital (NBO) and canonical molecular orbital analyses were used to examine orbital populations and interactions.[7] Adaptive natural density partitioning (AdNDP) was applied to identify localized and delocalized bonding patterns.[8] All NBO, canonical molecular orbital energy, and AdNDP analyses were performed at the PBE0/def2-TZVPP level. In parallel, electron density analysis was used to characterize bonding interactions based on the topology of the electron density.[9] Orbital composition analyses and electron density calculations were carried out using the Multiwfn

program.[10] The bonding character was further analyzed within the interacting quantum atoms (IQA) framework, which partitions interatomic interactions into electrostatic (V_C^{int}) and exchange–correlation (V_{XC}^{int}) contributions.[11]

Magnetic response was analyzed to evaluate possible aromatic contributions. The induced magnetic field ($\mathbf{B}^{ind}$) and current density ($\mathbf{J}^{ind}$) were computed at the DFT level using the BHandHLYP functional with the def2-TZVP basis set within the GIAO formalism.[12,13] The B^{ind}_z component was obtained using the Aromagnetic program, exploiting molecular symmetry.[14] The induced current density was also computed at the same level using the GIMIC program,[15,16] allowing qualitative analysis of current pathways.

All electronic structure calculations were performed with Gaussian 16.[17] IQA and energy decomposition analysis–natural orbitals for chemical valence (EDA–NOCV) were carried out using ADF 2023.[18,19]

References

1. M. Saunders, *J. Comput. Chem.*, 2004, **25**, 621–626.
2. C. Adamo and V. Barone, *J. Chem. Phys.*, 1999, **110**, 6158–6170.
3. F. Weigend and R. Ahlrichs, *Phys. Chem. Chem. Phys.*, 2005, **7**, 3297–3305.
4. S. Grimme, S. Ehrlich and L. Goerigk, *J. Comput. Chem.*, 2011, **32**, 1456–1465.
5. K. Raghavachari, G. W. Trucks, J. A. Pople and M. Head-Gordon, *Chem. Phys. Lett.*, 1989, **157**, 479–483.
6. J. M. Millam, V. Bakken, W. Chen, W. L. Hase and H. B. Schlegel, *J. Chem. Phys.*, 1999, **111**, 3800–3805.

7. A. E. Reed, R. B. Weinstock and F. Weinhold, *J. Chem. Phys.*, 1985, **83**, 735–746.

8. D. Y. Zubarev and A. I. Boldyrev, *Phys. Chem. Chem. Phys.*, 2008, **10**, 5207–5217.

9. R. F. W. Bader, *Chem. Rev.*, 1991, **91**, 893–928.

10. T. Lu and F. W. Chen, *J. Comput. Chem.*, 2012, **33**, 580–592.

11. M. A. Blanco, A. M. Pendás and E. Francisco, *J. Chem. Theory Comput.*, 2005, **1**, 1096–1109.

12. A. D. Becke, *J. Chem. Phys.*, 1993, **98**, 1372–1377.

13. K. Wolinski, J. F. Hinton and P. Pulay, *J. Am. Chem. Soc.*, 1990, **112**, 8251–8260.

14. F. Martínez-Villarino, M. Orozco-Ic and G. Merino, *Aromagnetic 2.0*; Cinvestav Mérida: Mérida, Mexico, 2025.

15. J. Jusélius, D. Sundholm and J. Gauss, *J. Chem. Phys.*, 2004, **121**, 3952–3963.

16. D. Sundholm, H. Fliegl and R. J. F. Berger, *WIREs Comput. Mol. Sci.*, 2016, **6**, 639–678.

17. M. J. Frisch *et al.*, *Gaussian 16*, Revision C.01, Gaussian, Inc., Wallingford, CT, 2016.

18. M. P. Mitoraj, A. Michalak and T. Ziegler, *J. Chem. Theory Comput.*, 2009, **5**, 962–975.

19. ADF2023, SCM, Theoretical Chemistry, Vrije Universiteit, Amsterdam, The Netherlands, http://www.scm.com.

Table S1. Lowest vibrational frequencies (ν_{min}, cm^{-1}) and the numbers of imaginary frequencies (N_{IMG}) for D_{5h} $FM_5E_5^-$ clusters (M = Be–Ba, Zn–Hg; E = O–Po) at the PBE0-D3(BJ)/def2-TZVPP level.

System	ν_{min}	N_{IMG}	System	ν_{min}	N_{IMG}
$FBe_5O_5^-$	141*i*	3	$FBa_5O_5^-$	isomerization	
$FBe_5S_5^-$	232*i*	6	$FBa_5S_5^-$	120*i*	10
$FBe_5Se_5^-$	259*i*	6	$FBa_5Se_5^-$	120*i*	9
$FBe_5Te_5^-$	280*i*	6	$FBa_5Te_5^-$	isomerization	
$FBe_5Po_5^-$	279*i*	6	$FBa_5Po_5^-$	121*i*	6
$FMg_5O_5^-$	111*i*	4	$FZn_5O_5^-$	52	0
$FMg_5S_5^-$	179*i*	6	$FZn_5S_5^-$	86*i*	6
$FMg_5Se_5^-$	185*i*	6	$FZn_5Se_5^-$	112*i*	6
$FMg_5Te_5^-$	191*i*	6	$FZn_5Te_5^-$	131*i*	6
$FMg_5Po_5^-$	191*i*	6	$FZn_5Po_5^-$	131*i*	6
$FCa_5O_5^-$	158*i*	6	$FCd_5O_5^-$	23*i*	2
$FCa_5S_5^-$	156*i*	6	$FCd_5S_5^-$	89*i*	6
$FCa_5Se_5^-$	158*i*	6	$FCd_5Se_5^-$	107*i*	6
$FCa_5Te_5^-$	161*i*	6	$FCd_5Te_5^-$	120*i*	6
$FCa_5Po_5^-$	162*i*	6	$FCd_5Po_5^-$	119*i*	6
$FSr_5O_5^-$	137*i*	9	$FHg_5O_5^-$	49*i*	1
$FSr_5S_5^-$	135*i*	6	$FHg_5S_5^-$	78*i*	6
$FSr_5Se_5^-$	137*i*	6	$FHg_5Se_5^-$	100*i*	6
$FSr_5Te_5^-$	138*i*	6	$FHg_5Te_5^-$	121*i*	6
$FSr_5Po_5^-$	138*i*	6	$FHg_5Po_5^-$	124*i*	6

Table S2. Lowest vibrational frequency (ν_{min}, in cm^{-1}) at seven theoretical levels for **1** (D_{5h}, $^1A_1$') of $F©Zn_5O_5^-$ cluster.

Level	ν_{min}
PBE0-D3(BJ)/def2-TZVPP	52
BP86-D3(BJ)/def2-TZVPP	49
B3LYP-D3(BJ)/def2-TZVPP	49
B3PW91-D3(BJ)/def2-TZVPP	52
TPSS-D3(BJ)/def2-TZVPP	52
ωB97X-D/def2-TZVPP	47
TPSSh/def2-TZVPP	54

Table S3. Electron density parameters (atomic units) at the bond critical points corresponding to interactions in the $F©Zn_5O_5^-$ cluster.

Interaction	$\rho(\boldsymbol{r})$	$\nabla^2\rho(\boldsymbol{r})$	H($\boldsymbol{r}$)	–G($\boldsymbol{r}$)/V($\boldsymbol{r}$)	Delocalization index
F–Zn	0.029	0.122	0.0004	1.014	0.15
Zn–O	0.134	0.651	–0.048	0.814	0.83

Table S4. IQA energy components for the D_{5h} F©$Zn_5O_5^-$ and Zn_5O_5 systems at the PBE0/TZ2P level. V_{IQA}^{int}, V_{C}^{int}, and V_{XC}^{int} denote the total interatomic interaction energy and its Coulombic and exchange-correlation energy components, respectively (kcal mol^{-1}).

	F©$Zn_5O_5^-$	Zn_5O_5
V_{IQA}^{int} (F–Zn)	–168.1	—
V_{C}^{int} (F–Zn)	–148.1 (88.1%)	—
V_{XC}^{int} (F–Zn)	–20.0 (11.9%)	—
V_{IQA}^{int} (Zn–Zn)	182.3	163.8
V_{C}^{int} (Zn–Zn)	185.9 (98.1%)	167.9 (97.6%)
V_{XC}^{int} (Zn–Zn)	–3.6 (1.9%)	–4.1 (2.4%)
V_{IQA}^{int} (Zn–O)	–392.5	–393.8
V_{C}^{int} (Zn–O)	–273.2 (69.6%)	–268.0 (68.1%)
V_{XC}^{int} (Zn–O)	–119.3 (30.4%)	–125.8 (31.9%)

Table S5. Mulliken population analysis of molecular orbitals (MOs) for the global minimum (**1**) of F©$Zn_5O_5^-$ at the PBE0/def2-TZVPP level. Molecular orbitals are visualized with an isosurface value of 0.03. Energies are given in eV.

CMO	F (%)		Zn_5 (%)		O_5 (%)	
	s/*p*	total	*s*/*p*/*d*	total	*s*/*p*	total
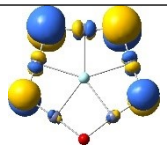 HOMO (e_2'') –0.13	0.0/0.0	0.0	0.0/0.0/12.6	12.6	0.0/87.4	**87.4**
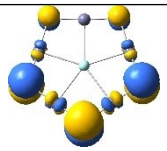 HOMO′ (e_2'') –0.13	0.0/0.0	0.0	0.0/0.0/12.5	12.5	0.0/**87.5**	**87.5**
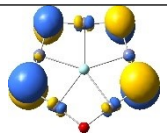 HOMO–1 (e_1'') –0.16	0.0/0.0	0.0	0.0/11.4/3.8	15.2	0.0/**84.8**	**84.8**
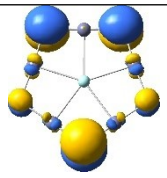 HOMO–1′ (e_1'') –0.16	0.0/0.0	0.0	0.0/11.1/4.1	15.2	0.0/**84.8**	**84.8**

CMO	F (%)		Zn_5 (%)		O_5 (%)	
	s/*p*	total	*s*/*p*/*d*	total	*s*/*p*	total
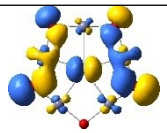 HOMO–2 (e_1') –0.16	0.0/15.7	15.7	15.0/0.0/7.8	**22.8**	0.0/**61.5**	**61.5**
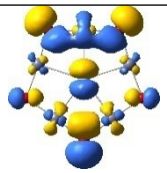 HOMO–2′ (e_1') –0.16	0.0/15.7	15.7	14.2/0.0/8.6	**22.8**	0.0/**61.5**	**61.5**
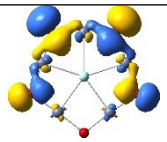 HOMO–3 (e_2') –0.16	0.0/0.0	0.0	1.8/4.7/8.3	14.8	0.0/**85.2**	**85.2**
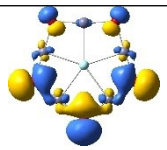 HOMO–3′ (e_2') –0.16	0.0/0.0	0.0	1.3/5.1/8.4	14.8	0.0/**85.2**	**85.2**
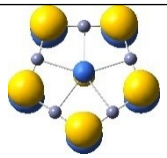 HOMO–4 (a_2'') –0.17	0.0/3.2	3.2	0.0/16.4/0.0	16.4	0.0/**83.6**	**83.6**

CMO	F (%)		Zn_5 (%)		O_5 (%)	
	s/*p*	total	*s*/*p*/*d*	total	*s*/*p*	total
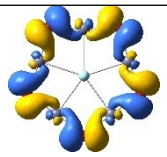 HOMO−5 (a_2') −0.18	0.0/0.0	0.0	0.0/11.6/5.4	17.0	0.0/**83.0**	**83.0**
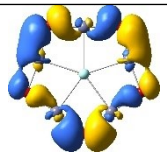 HOMO−6 (e_1') −0.20	0.0/0.0	0.0	13.4/10.2/3.3	**26.9**	0.0/**73.1**	**73.1**
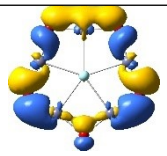 HOMO−6′ (e_1') −0.20	0.0/0.0	0.0	12.9/10.6/3.4	**26.9**	0.0/**73.1**	**73.1**
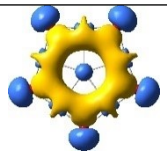 HOMO−7 (a_1') −0.20	0.8/0.0	0.8	**25.3**/7.8/3.3	**36.4**	0.0/**62.8**	**62.8**
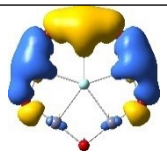 HOMO−8 (e_2')	0.0/0.0	0.0	**36.6**/2.8/11.8	**51.2**	0.0/**48.8**	**48.8**

CMO	F (%)		Zn_5 (%)		O_5 (%)	
	s/*p*	total	*s*/*p*/*d*	total	*s*/*p*	total
–0.22						
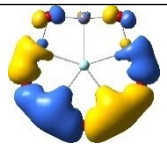 HOMO–8′ (e_2') –0.22	0.0/0.0	0.0	**36.0**/3.2/12.0	**51.2**	0.0/**48.8**	**48.8**
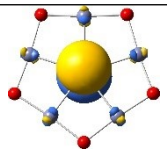 HOMO–9 (a_2'') –0.25	0.0/**94.0**	**94.0**	0.0/0.0/6.0	6.0	0.0/0.0	0.0
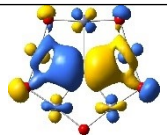 HOMO–10 (e_1') –0.28	0.0/**66.4**	**66.4**	7.6/4.1/13.3	**25.0**	0.0/8.6	8.6
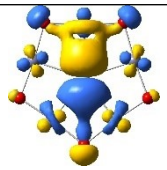 HOMO–10′ (e_1') –0.28	0.0/**66.4**	**66.4**	7.7/3.9/13.4	**25.0**	0.0/8.6	8.6

CMO	F (%)		Zn_5 (%)		O_5 (%)	
	s/*p*	total	*s*/*p*/*d*	total	*s*/*p*	total
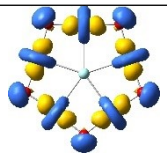 HOMO−11 (a_1') −0.36	0.0/0.0	0.0	0.0/0.0/**86.3**	**86.3**	0.0/13.7	13.7
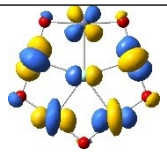 HOMO−12 (e_1') −0.36	0.0/2.4	2.4	1.1/0.0/**94.0**	**95.1**	1.4/1.1	2.5

CMO	F (%)		Zn_5 (%)		O_5 (%)	
	s/*p*	total	*s*/*p*/*d*	total	*s*/*p*	total
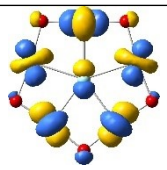 HOMO−12′ (e_1') −0.36	0.0/2.4	2.4	0.6/0.0/**94.6**	**95.2**	0.7/1.7	2.4
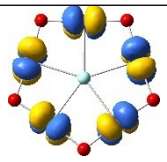 HOMO−13 (a_1'') −0.37	0.0/0.0	0.0	0.0/0.0/**100.0**	**100.0**	0.0/0.0	0.0

CMO	F (%)		Zn_5 (%)		O_5 (%)	
	s/*p*	total	*s*/*p*/*d*	total	*s*/*p*	total
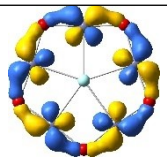 HOMO−14 (a_2') −0.37	0.0/0.0	0.0	0.0/0.0/**94.7**	**94.7**	0.0/5.3	5.3
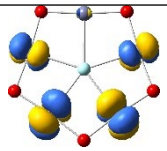 HOMO−15 (e_2'') −0.38	0.0/0.0	0.0	0.0/0.0/**100.0**	**100.0**	0.0/0.0	0.0
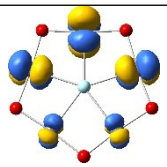 HOMO−15′ (e_2'') −0.38	0.0/0.0	0.0	0.0/0.0/**100.0**	**100.0**	0.0/0.0	0.0
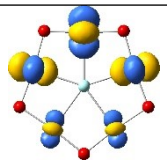 HOMO−16 (e_2') −0.38	0.0/0.0	0.0	0.0/0.0/**100.0**	**100.0**	0.0/0.0	0.0
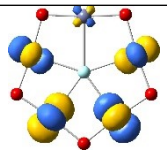 HOMO−16′ (e_2')	0.0/0.0	0.0	0.0/0.0/**100.0**	**100.0**	0.0/0.0	0.0

CMO	F (%)		Zn_5 (%)		O_5 (%)	
	s/*p*	total	*s*/*p*/*d*	total	*s*/*p*	total
–0.38						

CMO	F (%)		Zn_5 (%)		O_5 (%)	
	s/*p*	total	*s*/*p*/*d*	total	*s*/*p*	total
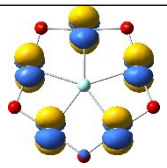 HOMO–17 (e_1'') –0.38	0.0/0.0	0.0	0.0/0.0/**100.0**	**100.0**	0.0/0.0	0.0
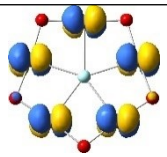 HOMO–17′ (e_1'') –0.38	0.0/0.0	0.0	0.0/0.0/**100.0**	**100.0**	0.0/0.0	0.0
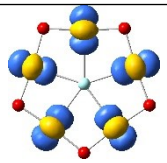 HOMO–18 (a_1') –0.38	0.0/0.0	0.0	0.0/0.0/**100.0**	**100.0**	0.0/0.0	0.0
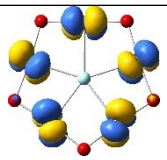 HOMO–19 (e_1'') –0.38	0.0/0.0	0.0	0.0/0.0/**100.0**	**100.0**	0.0/0.0	0.0
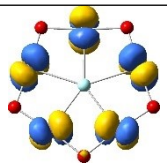 HOMO–19′ (e_1'')	0.0/0.0	0.0	0.0/0.0/**100.0**	**100.0**	0.0/0.0	0.0

CMO	F (%)		Zn_5 (%)		O_5 (%)	
	s/*p*	total	*s*/*p*/*d*	total	*s*/*p*	total
–0.38						
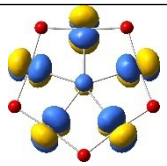 HOMO–20 (a_2'') –0.38	0.0/0.0	0.0	0.0/0.0/**100.0**	**100.0**	0.0/0.0	0.0
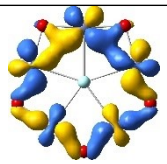 HOMO–21 (e_2') –0.38	0.0/0.0	0.0	0.0/0.0/**98.8**	**98.8**	0.0/1.2	1.2
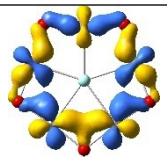 HOMO–21′ (e_2') –0.38	0.0/0.0	0.0	0.0/0.0/**98.8**	**98.8**	0.0/1.2	1.2
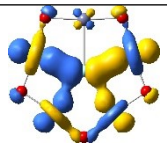 HOMO–22 (e_1') –0.39	0.0/6.0	6.0	0.0/0.0/**94.0**	**94.0**	0.0/0.0	0.0

CMO	F (%)		Zn_5 (%)		O_5 (%)	
	s/*p*	total	*s*/*p*/*d*	total	*s*/*p*	total
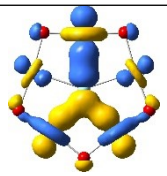 HOMO–22′ (e_1′) –0.39	0.0/6.0	6.0	0.0/0.0/**94.0**	**94.0**	0.0/0.0	0.0
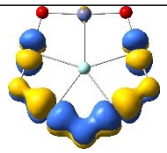 HOMO–23 (e_2″) –0.39	0.0/0.0	0.0	0.0/0.0/**94.4**	**94.4**	0.0/5.6	5.6
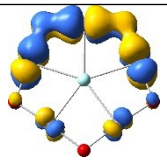 HOMO–23′ (e_2″) –0.39	0.0/0.0	0.0	0.0/0.0/**94.4**	**94.4**	0.0/5.6	5.6
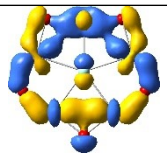 HOMO–24 (e_1′) –0.39	0.0/2.1	2.1	0.0/0.0/**87.0**	**87.0**	0.0/10.9	10.9
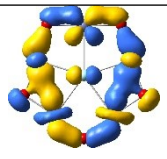 HOMO–24′ (e_1′)	0.0/2.1	2.1	0.0/0.0/**87.0**	**87.0**	0.0/10.9	10.9

CMO	F (%)		Zn_5 (%)		O_5 (%)	
	s/*p*	total	*s*/*p*/*d*	total	*s*/*p*	total
–0.39						

CMO	F (%)		Zn_5 (%)		O_5 (%)	
	s/*p*	total	*s*/*p*/*d*	total	*s*/*p*	total
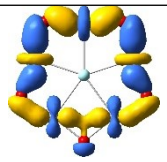 HOMO–25 (e_2') –0.40	0.0/0.0	0.0	0.0/0.0/**84.8**	**84.8**	0.0/15.2	15.2
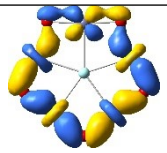 HOMO–25′ (e_2') –0.40	0.0/0.0	0.0	0.0/0.0/**84.8**	**84.8**	0.0/15.2	15.2
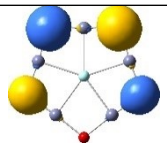 HOMO–26 (e_2') –0.77	0.0/0.0	0.0	0.0/7.1/0.0	7.1	**92.9**/0.0	**92.9**
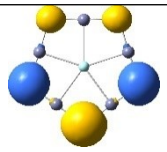 HOMO–26′ (e_2') –0.77	0.0/0.0	0.0	0.0/7.1/0.0	7.1	**92.9**/0.0	**92.9**
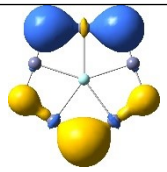 HOMO–27 (e_1')	0.0/0.0	0.0	7.8/2.6/6.5	16.9	**83.1**/0.0	**83.1**

CMO	F (%)		Zn_5 (%)		O_5 (%)	
	s/*p*	total	*s*/*p*/*d*	total	*s*/*p*	total
–0.78						
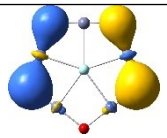 HOMO–27′ (e_1′) –0.78	0.0/0.0	0.0	8.5/3.3/5.0	16.8	**83.2**/0.0	**83.2**
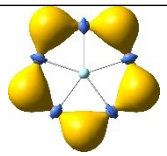 HOMO–28 (a_1′) –0.79	0.0/0.0	0.0	11.1/0.0/19.5	**21.4**	**78.6**/0.0	**78.6**

CMO	F (%)		Zn_5 (%)		O_5 (%)	
	s/*p*	total	*s*/*p*/*d*	total	*s*/*p*	total
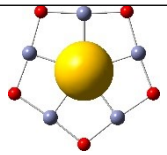 HOMO–29 (a_1') –0.99	**100.0**/0.0	**100.0**	0.0/0.0/0.0	0.0	0.0/0.0	0.0

Table S6. Energy decomposition analysis (EDA) results for **1** using F and Zn_5O_5 fragments in different charge and electronic states at the PBE0/TZ2P-ZORA level. All energy values are in kcal mol^{-1}.

Energy Term	F^- (singlet) + Zn_5O_5 (singlet)	F (doublet) + $Zn_5O_5^-$ (doublet)	F^+ (singlet) + $Zn_5O_5^{2-}$ (singlet)
ΔE_{int}	−106.8	−215.2	−852.3
ΔE_{Pauli}	103.9	91.6	84.1
ΔV_{elstat}	−151.1 (71.7%)	−53.4 (17.4%)	−184.6 (19.7%)
ΔE_{oi}	**−59.6** (28.3%)	−253.4 (82.6%)	−751.8 (80.3%)

Table S7. EDA–NOCV results of **1** using F^- and Zn_5O_5 as interacting fragments at the PBE0/TZ2P-ZORA level. All energy values are in kcal mol^{-1}.

Energy Term	Interaction	F^- (singlet) + Zn_5O_5 (singlet)
ΔE_{int}		−106.8
ΔE_{Pauli}		103.9
ΔV_{elstat}[a]		−151.1 (71.7%)
ΔE_{oi}[a]		−59.6 (28.3%)
$\Delta E_{oi(1)}$[b]	F^- (2*s*) → Zn_5O_5 donation	−15.3 (25.6%)
$\Delta E_{oi(2)}$[b]	F^- (2p_x) → Zn_5O_5 donation	−15.9 (26.7%)
$\Delta E_{oi(3)}$[b]	F^- (2p_y) → Zn_5O_5 donation	−15.9 (26.7%)
$\Delta E_{oi(rest)}$[b]		−12.5 (21.0%)

[a] The percentage contribution with respect to the total attraction is given in parentheses.

[b] The percentage contribution with respect to the total orbital interaction is given in parentheses.

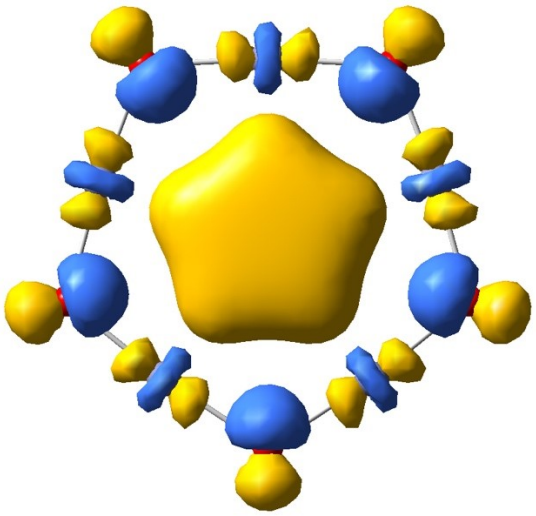

Figure S1. Lowest unoccupied molecular orbital (LUMO) of $F©Zn_5O_5^-$ computed at the PBE0/def2-TZVPP level. The isosurface value is 0.03.

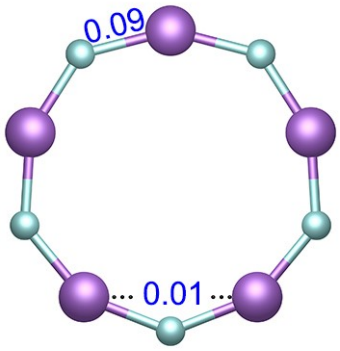

Figure S2. Wiberg bond indices (WBIs, blue) for Li_5F_5 at the PBE0-D3(BJ)/def2-TZVPP level.

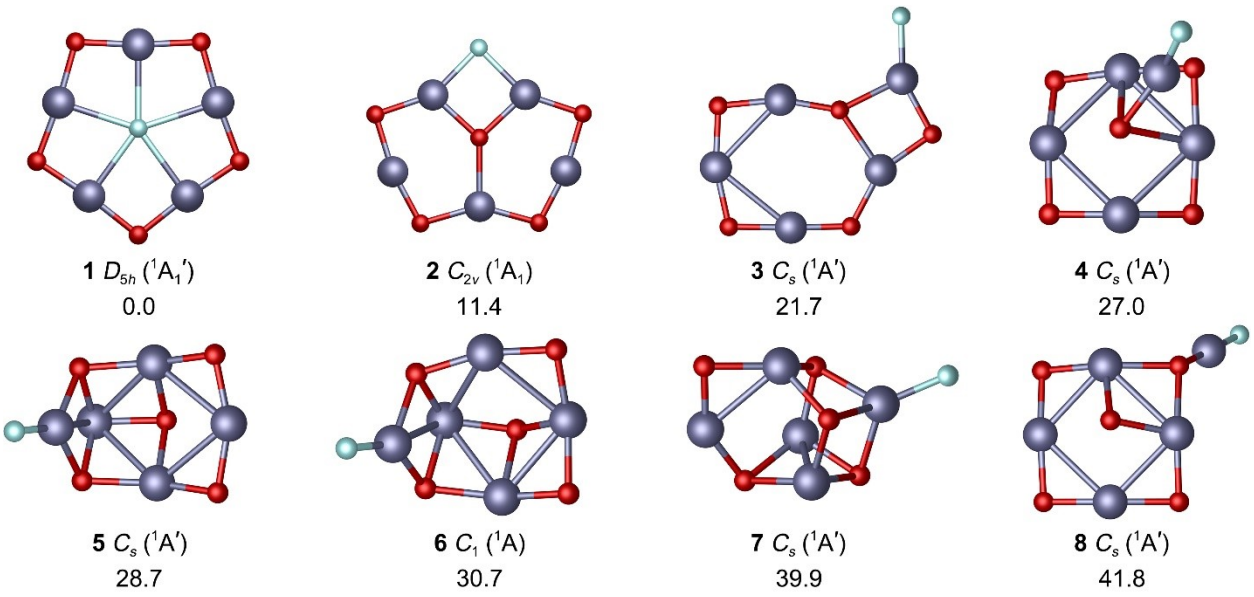

Figure S3. PBE0-D3(BJ)/def2-TZVPP geometries of the eight lowest-energy isomers of $FZn_5O_5^-$. Relative energies (kcal mol^{-1}) are given at the CCSD(T)/def2-TZVPP//PBE0-D3(BJ)/def2-TZVPP level, including zero-point energy corrections evaluated at the PBE0-D3(BJ)/def2-TZVPP level. The lowest-energy triplet structure lies 72.6 kcal mol^{-1} above structure **1** and is therefore not included.

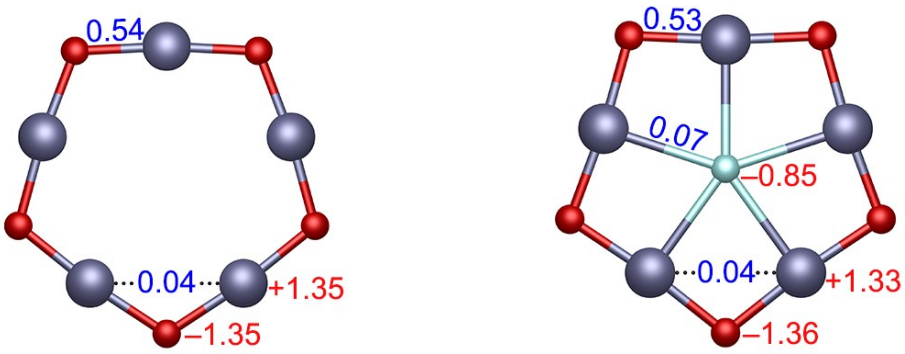

Zn_5O_5 (D_{5h}, $^1A_1'$) **1** F©$Zn_5O_5^-$ (D_{5h}, $^1A_1'$)

Figure S4. WBIs (blue) and natural atomic charges (|e|, red) for Zn_5O_5 and **1** at the PBE0-D3(BJ)/def2-TZVPP level.

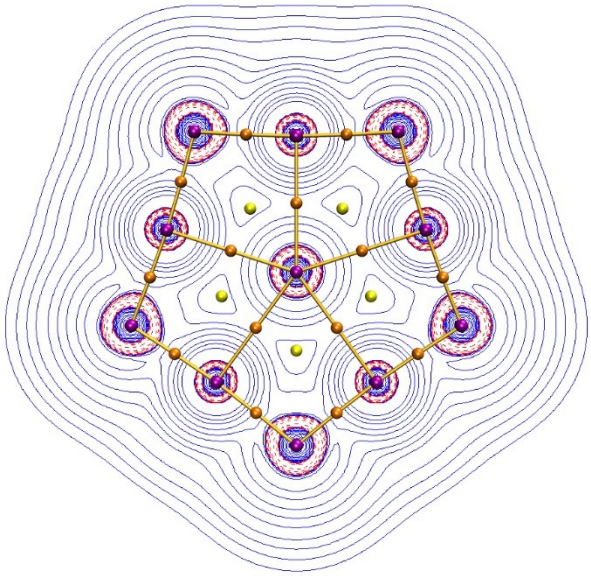

Figure S5. Laplacian of the electron density, bond paths, and bond and ring critical points for structure **1**. Regions of charge concentration ($\nabla^2\rho(r) < 0$) are indicated by red dashed contours, whereas regions of charge depletion ($\nabla^2\rho(r) > 0$) are shown in blue. Bond paths are represented by brown sticks; bond and ring critical points are marked by brown and yellow dots, respectively.

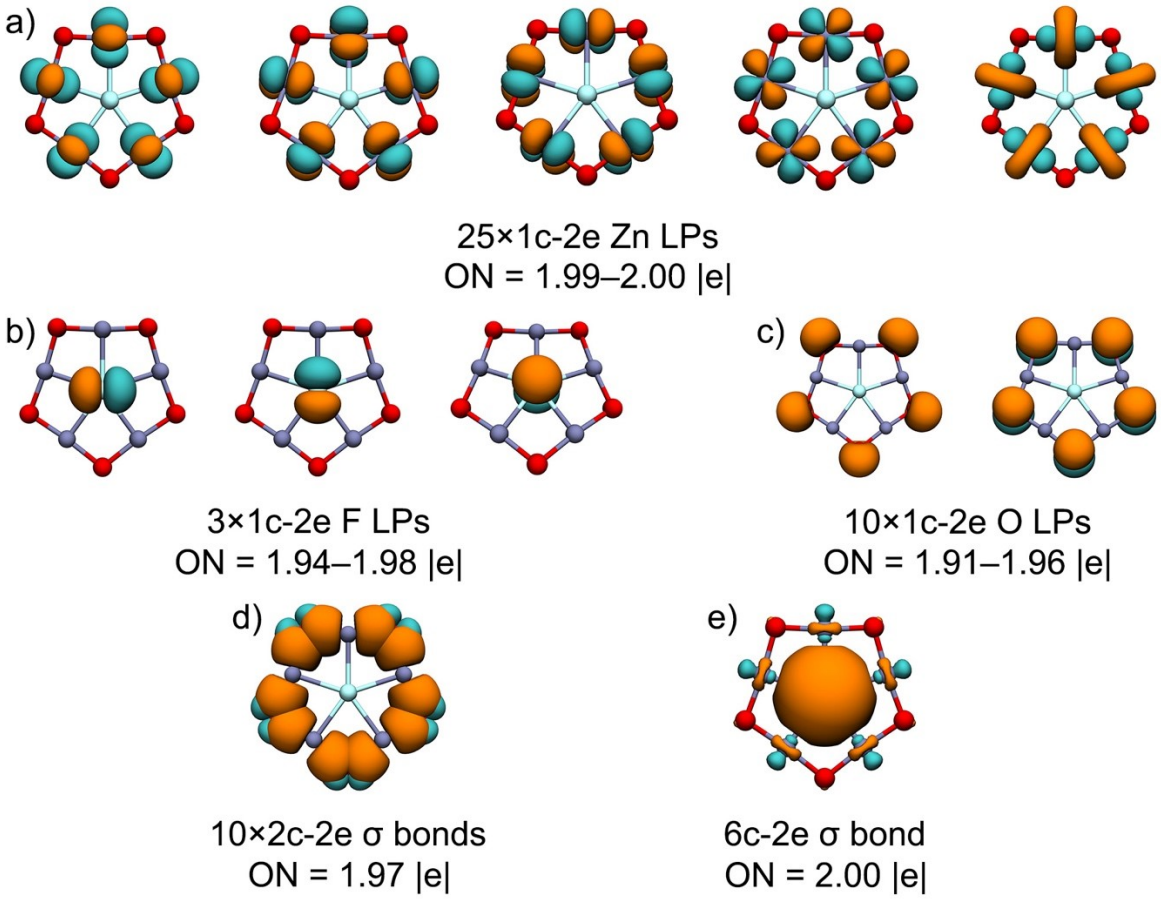

Figure S6. AdNDP bonding pattern of F©$Zn_5O_5^-$. Occupation numbers (ONs, in |e|) are indicated. a) Twenty-five lone pairs (LPs) localized on the Zn atoms; b) three LPs on the F atom; c) ten LPs on the O atoms; d) ten 2c–2e Zn–O σ bonds; e) one 6c–2e FZn_5 σ bond.

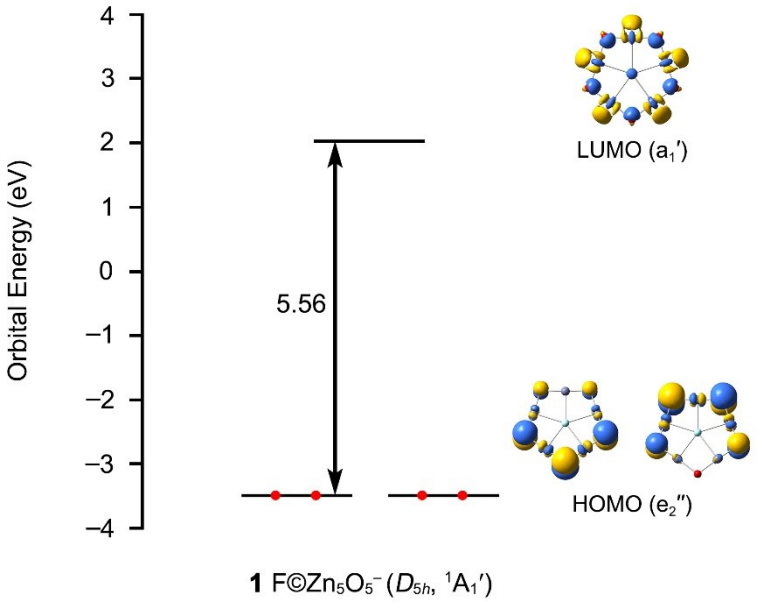

Figure S7. HOMO, LUMO, and HOMO–LUMO energy gap of 1 computed at the PBE0/def2-TZVPP level.

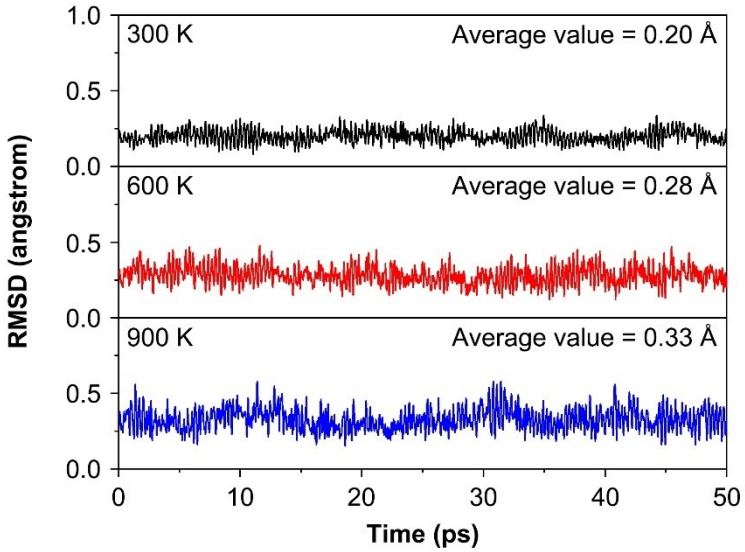

Figure S8. Root-mean-square deviations (RMSDs) of **1** during 50 ps Born–Oppenheimer molecular dynamics simulations at 300, 600 and 900 K, performed at the PBE0/def2-SVP level.

Cartesian coordinates of the top eight lowest-energy isomers of $FZn_5O_5^-$ optimized at the PBE0-D3(BJ)/def2-TZVPP level.

1 F©$Zn_5O_5^-$ (D_{5h}, $^1A_1'$)

F	0.00000000	0.00000000	0.00000000
Zn	0.00000000	2.38994000	0.00000000
Zn	2.27296800	0.73853200	0.00000000
Zn	-2.27296800	0.73853200	0.00000000
Zn	1.40477200	-1.93350200	0.00000000
Zn	-1.40477200	-1.93350200	0.00000000
O	2.89675400	-0.94121200	0.00000000
O	1.79029200	2.46412600	0.00000000
O	-1.79029200	2.46412600	0.00000000
O	-2.89675400	-0.94121200	0.00000000
O	0.00000000	-3.04582700	0.00000000

2 (C_{2v}, $^1A_1$)

F	0.00000000	-2.97269700	0.00000000
Zn	1.39576300	-1.55195200	0.00000000
Zn	2.61602300	0.75978600	0.00000000
Zn	-1.39576300	-1.55195200	0.00000000
Zn	0.00000000	1.82197300	0.00000000
Zn	-2.61602300	0.75978600	0.00000000
O	1.78867900	2.32352500	0.00000000
O	3.13296700	-0.96937700	0.00000000
O	-3.13296700	-0.96937700	0.00000000

O	-1.78867900	2.32352500	0.00000000
O	0.00000000	-0.25516400	0.00000000

3 (C_s, ^{1}A′)

F	-0.09146500	-4.44765000	0.00000000
Zn	-1.93107400	-0.33324200	0.00000000
Zn	-1.06818300	-2.91866900	0.00000000
Zn	1.61813100	-0.55025100	0.00000000
Zn	-0.59101500	2.45211100	0.00000000
Zn	2.18622100	2.09408800	0.00000000
O	-2.05615100	1.50649000	0.00000000
O	0.95591000	3.37341600	0.00000000
O	3.05674800	0.54183500	0.00000000
O	-2.65641100	-2.00847100	0.00000000
O	0.00000000	-1.19980400	0.00000000

4 (C_s, ^{1}A′)

F	1.77376913	-3.49247534	0.00000000
Zn	0.41292388	1.70963130	-1.32632989
Zn	-0.97346461	-0.53555040	1.34109881
Zn	-0.97346461	-0.53555040	-1.34109881
Zn	0.83837029	-1.96582423	0.00000000
Zn	0.41292388	1.70963130	1.32632989
O	-0.66967055	0.79498428	-2.50352107
O	0.95822611	2.84206496	0.00000000
O	-0.66967055	0.79498428	2.50352107
O	-1.28437039	-1.83687644	0.00000000

O	0.73016202	-0.09988823	0.00000000

5 (C_s, ^{1}A′)

F	2.46128200	-2.91935100	0.00000000
Zn	-0.26977000	0.51245400	1.55788000
Zn	-0.26977000	0.51245400	-1.55788000
Zn	0.91653600	-1.98563400	0.00000000
Zn	-1.56442000	-1.15016700	0.00000000
Zn	0.67134400	2.42543900	0.00000000
O	0.65411500	2.10592700	1.76679200
O	0.65411500	2.10592700	-1.76679200
O	-0.26977000	-1.41858900	-1.45960600
O	-1.60233900	0.73004700	0.00000000
O	-0.26977000	-1.41858900	1.45960600

6 (C_1, ^{1}A)

F	3.56763700	0.16482500	-1.63720400
Zn	-0.55659800	-1.78430300	-0.15794300
Zn	-0.28344400	1.89925600	-0.04454000
Zn	0.48479300	-0.12082200	1.55816000
Zn	2.21274300	-0.10969000	-0.48091900
Zn	-2.22983400	0.12128700	-0.47439800
O	-1.30011100	-0.45720200	1.30772800
O	1.27488300	-1.53019400	0.36941000
O	-2.00131200	-1.55712200	-1.25969400
O	-1.93918100	1.97208100	-0.66827900
O	1.34840600	1.36553100	0.59133400

7 (C_s, ^{1}A′)

F	-3.70463096	0.99764348	0.00000000
Zn	-2.00535805	0.32298126	0.00000000
Zn	-0.08745339	-1.07546927	1.24067964
Zn	0.49181711	1.58270893	0.00000000
Zn	-0.08745339	-1.07546927	-1.24067964
Zn	2.42993890	-0.04909333	0.00000000
O	-0.52726017	0.75541974	1.44909100
O	-1.44006131	-1.66580982	0.00000000
O	-0.52726017	0.75541974	-1.44909100
O	1.47479170	-1.58607220	0.00000000
O	2.40680913	1.72282568	0.00000000

8 (C_s, ^{1}A′)

F	-2.49972400	4.12498900	0.00000000
Zn	0.19518800	-2.08249400	1.33326100
Zn	0.19518800	-2.08249400	-1.33326100
Zn	0.56845500	0.45343200	-1.36149200
Zn	0.56845500	0.45343200	1.36149200
Zn	-1.17623800	2.97597100	0.00000000
O	0.19518800	1.88997700	0.00000000
O	1.37292400	-0.63634300	0.00000000
O	-0.05018500	-3.30377900	0.00000000
O	-0.01106300	-0.76624500	2.61595300
O	-0.01106300	-0.76624500	-2.61595300